Volume 24, No 2 | International Journal of Radiation Research, April 2026

Analysis of the value of contrast-enhanced ultrasound with CT imaging in the assessment of preoperative cervical lymph node metastases in papillary thyroid cancer

T. Yu[1#], L. Liu[2#], Z. Wang[2], R. Li[2], M. Zhang[2*], C. Liu[2*]

[1]Department of Ultrasonography, The First Affiliated Hospital of Yangtze University, Jingzhou, Hubei; and Department of Ultrasonography, Songzi People's Hospital, Songzi, Hubei, China
[2]Department of Ultrasonography, The First Affiliated Hospital of Yangtze University, Jingzhou, Hubei, China

► ***Original article***

Corresponding author:
Mei Zhang, M.M.
E-mail: *littlefish.love@163.com*

Received: July 2025
Final revised: August 2025
Accepted: September 2025

Int. J. Radiat. Res., April 2026; 24(2): 441-447

DOI: 10.61186/ijrr.24.2.21

Keywords: *Thyroid cancer, papillary, lymphatic metastasis, tomography, X-ray computed, ultrasonography, diagnostic imaging.*

#Tao Yu and Lei Liu contributed equally to this work.

ABSTRACT

Background: Cervical lymph node metastasis (CLNM) significantly influences the prognostic outcomes of papillary thyroid cancer (PTC), and accurate preoperative evaluation is essential. The aim of study was to evaluate contrast-enhanced ultrasound (CEUS) combined with computed tomography (CT) for diagnosing CLNM. ***Materials and Methods:*** Retrospective analysis of 120 PTC patients, categorizing them into metastatic (n=56) and non-metastatic (n=64) groups based on pathological confirmation of CLNM. The imaging characteristics and diagnostic accuracy of CEUS, CT, and their combination were estimate. P<0.05 indicates a significant difference. ***Results:*** Metastatic group exhibited significantly higher rates of CT features (granular calcification, cystic necrosis within lymph nodes, enhancement of lymph node margins, indistinct borders between lymph nodes and surrounding tissues, irregular lymph node morphology, lymph node length ≥5 mm) and CEUS features (hyper enhancement, centripetal perfusion, circumferential enhancement) than non-metastatic group (P<0.05). Metastatic lymph nodes also showed significantly higher marginal zone peak intensity (PI) (9.35±2.29 vs 5.54±2.15) and area under curve (AUC) (243.7±41.83 vs 164.2±34.86) (P<0.001). The lymph node detection rate of the combined diagnosis (95.31%) was significantly higher than that of single CEUS (82.81%) or CT (71.88%) (P<0.05). In addition, combined diagnosis was associated with higher sensitivity (90.6% vs. 87.5% vs. 85.9%), specificity (94.6% vs. 83.9% vs. 76.8%), and area under the receiver operating characteristic (ROC) curve (0.926 vs. 0.857 vs. 0.814) were also superior to single CEUS or CT. ***Conclusion:*** The combination of CEUS and CT enhances the preoperative diagnosis of CLNM in PTC.

INTRODUCTION

Accounting for roughly 80% to 90% of all instances, papillary thyroid carcinoma is the predominant type of thyroid cancer [1-3]. A key factor that adversely impacts the prognosis of PTC patients is CLNM, which occurs at a high frequency of 20%-90% despite the disease's typically indolent growth and good overall prognosis [4-6]. Precise preoperative evaluation of CLNM is essential for tailoring surgical plans, enhancing patient outcomes, and lowering recurrence risks [7-9]. Currently, the commonly used imaging methods in clinical practice include ultrasound, CT, magnetic resonance imaging (MRI), etc. The noninvasive nature, convenience, and absence of radiation make ultrasound the preferred imaging way for cervical lymph node assessment. It can clearly show the bulk, form, border, internal structure and blood flow signal of lymph nodes [10-12]. However, conventional ultrasound may be affected by subjective factors in some cases, and there may be some underdiagnoses of small, early lymph node metastases or lymph node lesions with low contrast with surrounding tissues [13-15]. CT scanning can provide cross-sectional anatomical images, which are good for evaluating the distribution of cervical lymph nodes, their relationship with the surrounding tissues, and the presence or absence of fusion, but its sensitivity to subtle structural changes within the lymph nodes is relatively low, and there is a certain amount of radiation dose [16-18]. Contrast-enhanced ultrasound (CEUS) has emerged as a novel method for evaluating the thyroid and cervical lymph nodes. By injecting contrast material intravenously, CEUS enables real-time observation of thyroid and lymph node perfusion, enhancing the contrast between tissues and lesions, it aids in identifying microvascular changes within minute lesions and early metastatic lymph nodes that are undetectable with conventional ultrasound [19, 20]. The combined application of CEUS and CT imaging is expected to give full play to the advantages of the two imaging techniques, realize complementary advantages, and enhance the diagnostic accuracy and sensitivity of preoperative CLNM in PTC.

A number of studies have examined the role of

[DOI: 10.61186/ijrr.24.2.21]

CEUS or CT imaging alone in the diagnosis of thyroid disease [21-24]. However, studies on the combined application of the two in the evaluation of preoperative CLNM in PTC are still in the stage of continuous exploration and validation. The study is aim to comprehensively evaluate the value and efficacy of CEUS together with CT imaging in the diagnosis of CLNM by retrospectively analyzing the clinical data of patients with PTC, so as to provide scientific basis and theoretical support for further optimizing the preoperative diagnostic process and increasing the effectiveness of operation treatment for PTC. The study is the first to comprehensively integrate the functional perfusion characteristics of CEUS and the detailed morphological features of CT, establishing a more accurate and comprehensive preoperative lymph node assessment method. The findings not only validate the complementary advantages of CEUS and CT but also propose a practical imaging strategy that enhances clinical decision-making for patients with PTC.

MATERIALS AND METHODS

Patients

The data of 120 patients who underwent preoperative CEUS and CT in our hospital from January 2022 to January 2024 and were pathologically diagnosed as PTC were retrospectively selected. All patients received central neck lymph node dissection. When preoperative CEUS or CT indicated suspicious lymph nodes in the lateral neck region, dissection was also performed in the corresponding areas. Postoperative pathological findings served as the gold standard for determining the presence of cervical lymph node metastasis. According to the pathological findings, the patients were sorted into two groups: 56 cases with metastasis and 64 cases without metastasis. Ethical approval for the study was obtained from the Ethics Committee of the First Affiliated Hospital of Yangtze University (YYLL-2022015).

Inclusion and exclusion criteria

Inclusion criteria: (1) the diagnosis of papillary thyroid carcinoma was diagnosed as by pathological examination in all enrolled patients; (2) all patients underwent CEUS examination as well as CT examination; (3) intraoperative prophylactic central neck lymph node dissection (LND) or therapeutic central or lateral neck zone LND; (4) no previous invasive surgery, radiotherapy or chemotherapy in the neck. Exclusion criteria: (1) patients with limited clinical information available; (2) patients with concurrent malignant tumors at other sites; (3) patients with infectious conditions; (4) patients with hematopoietic system diseases; (5) patients with mental disorders and communication disorders.

Imaging methods

CT examination: a GE Revolution 256-row spiral CT scanner (General Electric Company, USA) was used to perform a CT-enhanced scan of the patient. The patients were injected with contrast agent iohexol (Omnipaque®, GE Healthcare, USA) 60-70mL, pushed intravenously at an injection rate of 3mL/s, and the thickness of the scanning layer was 0.625mm, and then the number, morphology, and location of the patients' lymph nodes were observed. CEUS examination: a diagnostic color Doppler ultrasound (GE LOGIQE9, General Electric Company, USA; Philips EPIQ7C, Philips Healthcare, Netherlands) was used for the examination, with a wire-array probe L5-12 at 12 MHz. First use conventional ultrasound to show the best viewed section of the lymph node, enter the ultrasonography mode, adjust the depth and gain parameters of the image, and observe the section containing the intact lesion and the surrounding normal tissue. The patient was instructed to breathe calmly during the examination and to avoid swallowing maneuvers.2.0 mL of Sonazoid (GE Healthcare, Norway) contrast agent was infused intravenously into the patient, then administer 5 mL of 0.9% saline to flush the tube, and the contrast agent was injected and stored in the dynamic image, recording the ultrasonographic performance of the lymph node lesion for more than 60 seconds (figure 1).

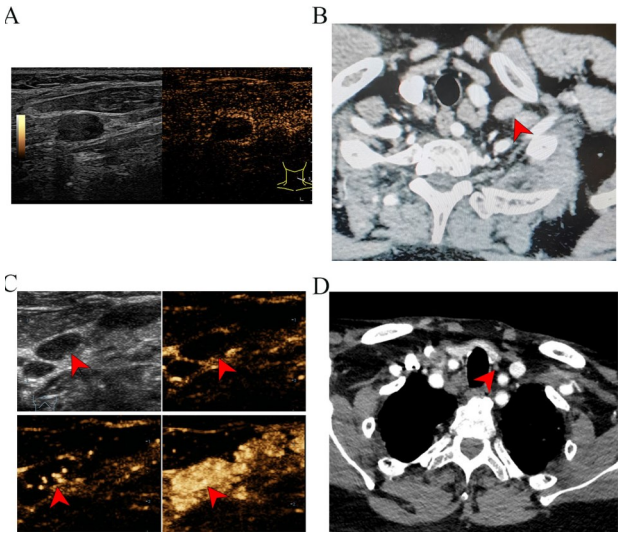

Figure 1. Preoperative imaging of a 38-year-old female patient with papillary thyroid carcinoma. **A:** Contrast-enhanced ultrasound (CEUS) image of a metastatic lymph node in the left neck shows circular enhancement; **B:** CT image of the metastatic lymph node in the left neck shows a regularly shaped lymph node with granular calcification, endocystic necrosis, and peripheral enhancement; **C:** CEUS images of a benign lymph node in the central region at 10s (C2), 13s (C3), and 17s (C4) demonstrate centrifugal perfusion and homogeneous enhancement; **D:** CT image of the benign lymph node in the central region shows clear boundaries and no granular calcification or endocystic necrosis.

[DOI: 10.61186/ijrr.24.2.21]

Observation indicators

(1) Positive lymph node diagnosis by three different diagnostic modalities: CT, CEUS and combined diagnosis. (2) Characterization of CT and CEUS in the two groups of patients. (3) The quantitative parameters related to CEUS, the main recording items include mean transit time (MTT), peak intensity (PI), rising time (RT), area under the curve (AUC), time to peak height (TPH), wash-in slope (WIS) and time to peak (TTP). (4) The value efficacy of CT, CEUS, and co-diagnosis.

Statistical analysis

Statistical analysis and graph generation were performed using GraphPad Prism 8.0 software (USA). Normally distributed measurement data are presented as mean ± standard deviation and compared using the t-test. Categorical data are expressed as number of cases (percentage), and group comparisons were carried out with the chi-square test; when the theoretical frequency in the chi -square test was below 5, Fisher's exact test was applied. The diagnostic performance of CEUS, CT, and their combination in detecting CLNM was estimated using the area under the receiver operating characteristic (ROC) curve (AUC). $P<0.05$ indicates a significant difference.

RESULTS

General data

The sum of 120 patients were included in the study.56 patients with PTC had metastatic lymph nodes (metastatic group), 22 males (39.29%), 34 females (60.71%), mean age (44.15 ± 8.60) years.64 patients had no metastatic lymph nodes (non-metastatic group). There were 26 males (40.62%) and 38 females (59.38%) with a mean age of (42.75 ± 8.31) years. The results showed that the clinical and pathological characteristics data of the two groups, such as age, gender, tumor size, capsular invasion, tumor node metastasis (TNM) stage, location of primary lesions, and number of primary lesions, did not show any significant difference upon comparison ($P>0.05$) (table 1).

Metastatic lymph node positivity rate

Pathologic diagnosis detected 128 positive lymph nodes, of which 92 (71.88%) were detected by CT, 106 (82.81%) were detected by CEUS, and 122 (95.31%) were detected by combined examination. The positive rate of CEUS examination was greater than that of CT examination ($P=0.037$), and the positive rate of combined examination was greater than that of CEUS examination ($P=0.001$) (table 2).

Characterization of CT and CEUS

CT features showed granular calcification (29.35% vs. 11.11%), cystic necrosis within lymph nodes (32.61% vs. 13.89%), enhancement of lymph node margins (31.52% vs. 8.33%), unclear borders between lymph nodes and surrounding tissues (39.13% vs. 19.44%), irregular lymph node morphology (41.30% vs. 22.22%), and lymph node length ≥5 mm (35.87% vs. 13.89%) were significantly greater in the metastatic group than in the non-metastatic group ($P<0.05$) (table 3). CEUS features showed that 36 metastatic lymph nodes were hyper-enhanced (64.29%), whereas only 15 of the non-metastatic lymph nodes were hyper-enhanced (17.9%); 29 metastatic lymph nodes had a centripetal perfusion pattern (51.79%), whereas only 21 of the non-metastatic lymph nodes were centripetal perfused (32.81%); and circular enhancement was visible in 19 metastatic lymph nodes under CEUS (33.93%), while ring enhancement was seen in only 5 cases of non-metastatic lymph nodes (7.81%). The two groups differed significantly in contrast enhancement pattern, perfusion pattern, and annular enhancement ($P<0.05$); whereas no significant difference was detected in enhancement types ($P=0.807$) (table 4).

Table 1. Comparison of clinical and pathological characteristics between the two groups.

Characteristic	CLNM group (n = 56)	Non-CLNM group (n = 64)	P value
Age (years)	44.15 ± 8.60	42.75 ± 8.31	0.372
Gender, n (%)			0.881
Female	34 (60.71)	38 (59.38)	
Men	22 (39.29)	26 (40.62)	
Tumor size (cm)	1.67 ± 0.47	1.59 ± 0.41	0.343
Capsular invasion, n (%)	36 (64.29)	32 (50.00)	0.115
TNM stage, n (%)			
T1	30 (53.57)	40 (62.50)	0.322
T2	16 (28.57)	18 (28.13)	0.957
T3	10 (17.86)	6 (9.37)	0.173
Location of primary lesion			
Left lobe	23 (41.07)	29 (45.31)	0.640
Right lobe	28 (50.00)	27 (42.19)	0.392
Bilateral lobe	5 (8.93)	8 (12.50)	0.571
Number of primary lesions, n (%)			0.922
Number of single lesions	24 (42.86)	28 (43.75)	
Number of multifocal lesions	32 (57.14)	36 (56.25)	

CLNM: cervical lymph node metastasis; TNM: tumor node metastasis.

Table 2. Comparison of detection rates of metastatic lymph nodes using CT, contrast-enhanced CEUS, and their combination.

Classification	Lymphatic node (n)	Metastasis positive lymph nodes (n)	Diagnostic positivity rate (%)
CT	128	92	71.88
CEUS	128	106	82.81
CT+CEUS	128	122	95.31
$\chi 2$			4.369 / 10.27
P value			0.037^a / 0.001^b

CT: Computed Tomography; CEUS: Contrast-enhanced ultrasound; a: Comparison of the positivity rate of CT and CEUS examinations; b: Comparison of the positivity rate of CEUS and CT+CEUS examinations.

[DOI: 10.61186/ijrr.24.2.21]

Table 3. Comparison of CT imaging features between metastatic and non-metastatic cervical lymph node groups [n (%)].

Classification	CLNM group	Non-CLNM group	χ2	P value
Lymphatic node	92 (71.88)	36 (28.12)		
Granular calcification	27 (29.35)	4 (11.11)	4.689	0.030
Endocystic necrosis of lymph nodes	30 (32.61)	5 (13.89)	4.564	0.033
Enhancement of lymph node margins	29 (31.52)	3 (8.33)	7.420	0.006
Lymph nodes and surrounding tissue			4.495	0.034
Clear boundaries	56 (60.87)	29 (80.56)		
Unclear boundary	36 (39.13)	7 (19.44)		
Lymph node morphology			4.092	0.043
Regularly	54 (58.70)	28 (77.78)		
Irregularly	38 (41.30)	8 (22.22)		
Lymph node longitudinal line			5.989	0.014
<5 mm	59 (64.13)	31 (86.11)		
≥5 mm	33 (35.87)	5 (13.89)		

CT: Computed Tomography; CLNM: cervical lymph node metastases.

Table 4. Comparison of CEUS enhancement patterns between metastatic and non-metastatic cervical lymph node groups [n (%)].

Classification	CLNM group (n = 56)	Non-CLNM group (n = 64)	χ2	P value
Contrast-enhanced mode			20.39	<0.001
Highly enhanced	36 (64.29)	15 (23.44)		
Equal or low enhancement	20 (35.71)	49 (76.56)		
Type of enhancement			0.060	0.807
Inhomogeneous enhancement	25 (44.64)	30 (46.88)		
Homogeneous enhancement	31 (55.36)	34 (53.13)		
Perfusion mode			4.423	0.035
Centripetal perfusion	29 (51.79)	21 (32.81)		
Centrifugal perfusion	27 (48.21)	43 (67.19)		
Circular enhancement			12.73	<0.001
Yes	19 (33.93)	5 (7.81)		
No	37 (66.07)	59 (92.19)		

CEUS: Contrast-enhanced ultrasound; CLNM: cervical lymph node metastases.

Quantitative parametric analysis of CEUS

A comparison of the two groups revealed no statistically significant differences in the parameters RT, MTT, TPH, WIS, and TTP (P > 0.05). The marginal zone PI (9.35 ± 2.29 vs. 5.54 ± 2.15, P < 0.001) and marginal zone AUC (243.7 ± 41.83 vs. 164.2 ± 34.86, P < 0.001) in the metastatic group were significantly greater than those in the non-metastatic group (table 5).

Diagnostic effectiveness assessment

Using pathologic examination as the gold standard, the sensitivity (90.6% vs. 87.5% vs. 85.9%) and specificity (94.6% vs. 83.9% vs. 76.8%) of the combined diagnosis were significantly higher than those of CEUS examination and CT examination. In addition, ROC curve analysis showed that the AUC of combined diagnosis (AUC: 0.926, 95%CI: 0.810-0.956) was higher than that of single CEUS (AUC: 0.857, 95%CI: 0.772-0.935) and CT examination (AUC: 0.814, 95%CI: 0.754-0.924) (table 6 and figure 2).

Table 5. Comparison of quantitative CEUS parameters between metastatic and non-metastatic cervical lymph node groups (mean ± SD).

Classification	CLNM group (n = 56)	Non-CLNM group (n = 64)	t	P value
RT (s)				
Marginal area	2.96 ± 1.03	3.40 ± 1.68	1.684	0.095
Central District	4.48 ± 1.64	3.93 ± 1.51	1.923	0.057
PI (dB)				
Marginal area	9.35 ± 2.29	5.54 ± 2.15	9.402	<0.001
Central District	4.32 ± 2.15	4.02 ± 2.05	0.776	0.439
MTT (s)				
Marginal area	9.58 ± 4.23	10.25 ± 4.02	0.899	0.371
Central District	10.19 ± 4.14	9.57 ± 4.71	0.765	0.446
AUC (dBs)				
Marginal area	243.7 ± 41.83	164.2 ± 34.86	11.35	<0.001
Central District	93.98 ± 42.73	86.96 ± 33.84	1.003	0.318
TPH (s)				
Marginal area	12.04 ± 5.20	13.23 ± 5.66	1.195	0.234
Central District	12.31 ± 5.21	11.61 ± 4.90	0.762	0.448
WIS (dB/s)				
Marginal area	3.23 ± 1.54	2.90 ± 1.54	1.164	0.247
Central District	2.26 ± 1.14	1.90 ± 1.03	1.822	0.071
TTP (s)				
Marginal area	13.43 ± 3.59	14.16 ± 4.16	1.024	0.308
Central District	13.64 ± 3.62	14.93 ± 3.99	1.847	0.067

CEUS: Contrast-enhanced ultrasound; CLNM: cervical lymph node metastases; RT: rising time; PI: peak intensity; MTT: mean transit time; AUC: area under curve; TPH: time to peak height; WIS: wash-in slope; TTP: time to peak.

Table 6. Diagnostic performance of CT, CEUS, and combined CT+CEUS for detecting cervical lymph node metastasis in papillary thyroid cancer.

Classification	CT	CEUS	CT+CEUS
AUC (95% CI)	0.814 (0.754-0.924)	0.857 (0.772-0.935)	0.926 (0.810-0.956)
Standard error	0.042	0.037	0.027
P	<0.001	<0.001	<0.001
Youden index	0.627	0.714	0.852
Sensitivity (%)	85.9	87.5	90.6
Specificity (%)	76.8	83.9	94.6

CT: Computed Tomography; CEUS: Contrast-enhanced ultrasound; AUC: area under curve; CI: confidence interval.

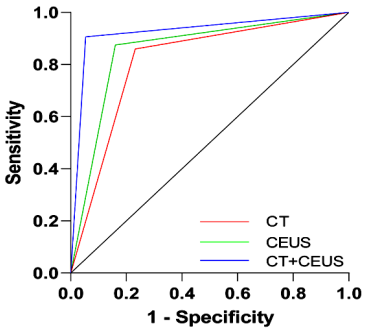

Figure 2. ROC curves of CT, CEUS and combined CT+CEUS for the assessment of cervical lymph node metastases occurring in papillary thyroid carcinoma.

DISCUSSIONS

In this study, the synergistic value of CEUS

[DOI: 10.61186/ijrr.24.2.21]

together with CT imaging in the diagnosis of CLNM was systematically evaluated for the first time by retrospectively analyzing the imaging and pathology data of 120 PTC patients. The results showed that the lymph node detection rate of combined diagnosis was significantly greater than that of single CEUS or CT ($P<0.05$), and the sensitivity, specificity and area under the ROC curve of combined diagnosis were better than that of single examination. This finding provides strong support for imaging strategies to optimize preoperative staging of PTC.

The core advantage of CEUS is the real-time dynamic assessment of lymph node microvascular perfusion. In this study, we found that metastatic lymph nodes mostly showed hyper improvement, centripetal perfusion and circumferential improvement in CEUS. These features are closely related to the abnormal proliferation of neovascularization and enrichment of marginal blood supply in the metastatic foci [25, 26]. Tumor cells promote neovascularization in the marginal zone through other factors such as vascular endothelial growth factor, leading to enhanced perfusion [27, 28]. Whereas centripetal perfusion patterns may arise from hemodynamic changes in metastatic foci infiltrating from the sub peritoneal sinus of lymph nodes to the medulla oblongata [29, 30]. In addition, ring enhancement suggests peritumoral vascular proliferation, a specific marker for identifying metastasis [31]. Notably, compared to the non-metastasis group, the metastasis group demonstrated significantly elevated PI and AUC values in the marginal zone ($P<0.001$), suggesting that the microvessel density of the marginal zone versus the volume of blood flow is an important quantitative index for identifying metastasis [32, 33]. However, CEUS has limitations in displaying deep lymph nodes or areas with complex anatomy. CT feature analysis in this study showed that the metastatic group had a significantly greater incidence of granular calcification, cystic necrosis within the lymph nodes, lymph node margin enhancement, unclear borders between the lymph nodes and the surrounding tissues, irregular lymph node morphology, and lymph node longitudinal lines ≥5 mm than the non-metastatic group ($P<0.05$). These features reflected the morphological and pathophysiological changes after lymph node metastasis. For example, granular calcification may be the result of tumor cell necrosis, degeneration, and calcium salt deposition [34]. Cystic necrosis in the lymph node suggests rapid tumor growth and relative lack of blood supply leading to necrotic liquefaction in the central area [35]. Enhancement of lymph node margins may be associated with tumor neovascularization [36]. Lymph nodes with unclear boundaries with surrounding tissues, irregular morphology, and increased longitudinal lines are signs of increased size and structural damage after lymph node metastasis [37]. Although CT compensates for the limitations of CEUS in displaying deep lymph nodes or areas with complex anatomy, CT is less sensitive to microvascular changes and tends to miss early metastases.

CEUS and CT have their own advantages in evaluating CLNM, but it is often difficult for a single imaging method to comprehensively and accurately assess lymph node metastasis [38-40]. The meta-analysis of Suh and Cho also pointed out that CT has certain diagnostic efficacy in diagnosing PTC lymph node metastasis, but there are still limitations, suggesting the need for multimodal imaging combination [21, 22]. CEUS identifies microvascular abnormalities, and CT localizes the extent of the lesion in relation to the surrounding tissues, and the combination of the two realizes a two-dimensional assessment of the functional perfusion and anatomical structure, which significantly reduces the rate of diagnosis leakage [41, 42]. For patients with the risk of lateral CLNM, the combined imaging examination can detect potential metastases in advance, enabling the surgeon to perform simultaneous lateral cervical lymph node dissection, optimizing the surgical process and improving the therapeutic effect. In addition, accurate preoperative evaluation also helps doctors to fully communicate with patients, so that patients have a clearer understanding of the surgical plan and prognosis, and enhance the compliance of treatment.

Limitations

This study has some limitations. As a retrospective single-center study, there may be potential selection and information biases that affect the accuracy and reliability of the results. The sample size included is relatively limited, which may restrict the generalizability of the findings. Additionally, this study did not perform subgroup analyses on the imaging differences of central and lateral CLNM. Further validation of these findings will require future multi-center prospective studies with larger sample sizes.

CONCLUSION

CEUS combined with CT imaging significantly improved the diagnostic accuracy of preoperative CLNM in PTC by integrating functional perfusion and morphologic features of lymph nodes. This combined strategy provides a reliable basis for individualized surgical decision-making for PTC and is expected to further improve patients' prognosis and quality of life.

***Acknowledgment*:** Not applicable.

***Conflict of Interest*:** The authors declare that there is no competing interest associated with the

[DOI: 10.61186/ijrr.24.2.21]

manuscript.

***Funding Statement*:** Not applicable.

***Availability of Data and Materials*:** The datasets used and/or analysed during the current study available from the corresponding author on reasonable request.

***Consent for publication*:** All the authors agree to publish this manuscript.

***Informed consent statement*:** All the selected patients were informed and agreed to the study and provided an informed consent to participate.

***Ethics statement*:** This study was approved by the Ethics Committee of The First Affiliated Hospital of Yangtze University. And the study was conducted in strict accordance with the Declaration of Helsinki and relevant ethical guidelines. The research content involved in this research meets the requirements of medical ethics and academic morality of our hospital, and the research content is reasonable, the risks are controllable, and there are no violations. The relevant research carried out is in line with the safe, standardized and true scientific research guiding principles, and in line with the requirements of the clinical research ethics code.

***Authors' contribution*:** T.Y. and L.L.: Conceptualization, methodology, formal analysis, investigation, data curation, writing - original draft. Z.W.: Software, validation, investigation, resources, visualization. R.L.: Supervision, project administration, writing - review & editing. M.Z. and C.L.: Conceptualization, resources, supervision, writing - review & editing, funding acquisition.

***AI usage statement*:** No AI generation technology was used in the writing of this paper, and all content was done independently by the author.

REFERENCES

1. Harahap AS and Jung CK (2024) Cytologic hallmarks and differential diagnosis of papillary thyroid carcinoma subtypes. *J Pathology and Translational Medicine,* ***58****(6): 265-82*.
2. Wang J, Yan M, Liu H, *et al.* (2024) Decoding the past and future of distant metastasis from papillary thyroid carcinoma: a bibliometric analysis from 2004 to 2023. *Frontiers in Oncology,* ***14****: 1432879*.
3. Carnazza M, Quaranto D, DeSouza N, *et al.* (2025) The Current understanding of the molecular pathogenesis of papillary thyroid cancer. *Int J Molecular Sciences,* ***26****(10): 4646*.
4. Xiuming L and Fuxing L (2024) Study on the effectiveness and accuracy of ultrasound diagnosis and pathological diagnosis of thyroid lesions. *Int J Radiat Res,* ***22****(3): 727*.
5. Dai L, Zheng L, Li Y, *et al.* (2025) Analysis and prediction of contralateral central lymph node metastasis risk in unilateral papillary thyroid carcinoma with ipsilateral lateral cervical lymph node: a retrospective clinical study. *Gland Surgery,* ***14****(3): 380-90*.
6. Liu Y, Wang Y, Zhao K, *et al.* (2020) Lymph node metastasis in young and middle-aged papillary thyroid carcinoma patients: a SEER-based cohort study. *BMC Cancer,* ***20****(1): 181*.
7. Haugen BR, Alexander EK, Bible KC, *et al.* (2015-6) American thyroid association management guidelines for adult patients with thyroid nodules and differentiated thyroid cancer: The American thyroid association guidelines task force on thyroid nodules and differentiated thyroid cancer. *Thyroid: Official Journal of the American Thyroid Association,* ***26****(1): 1-133*.
8. Ito Y, Miyauchi A, Kudo T, *et al.* (2017) The effectiveness of prophylactic modified neck dissection for reducing the development of lymph node recurrence of papillary thyroid carcinoma. *World Journal of Surgery,* ***41****(9): 2283-9*.
9. Tong Y, Li J, Huang Y, *et al.* (2021) Ultrasound-based radiomic nomogram for predicting lateral cervical lymph node metastasis in papillary thyroid carcinoma. *Academic Radiology,* ***28****(12): 1675-84*.
10. Ahuja A and Ying M (2003) Sonography of neck lymph nodes. Part II: abnormal lymph nodes. *Clinical Radiology,* ***58****(5): 359-66*.
11. Xie C, Cox P, Taylor N, *et al.* (2016) Ultrasonography of thyroid nodules: a pictorial review. *Insights into Imaging,* ***7****(1): 77-86*.
12. Wang X, Qi Y, Zhang X, *et al.* (2025) Ultrasound-based artificial intelligence for predicting cervical lymph node metastasis in papillary thyroid cancer: a systematic review and meta-analysis. *Frontiers in Endocrinology,* ***16****: 1570811*.
13. Jayapal N, Ram SKM, Murthy VS, *et al.* (2019) Differentiation between benign and metastatic cervical lymph nodes using ultrasound. *J Pharmacy & Bioallied Sciences,* ***11****(2): S338-s46*.
14. Gao J, Liu Y, Zheng L, *et al.* (2025) Diagnostic performance of contrast-enhanced ultrasound vs. conventional ultrasound for lymph node metastasis in patients with thyroid cancer: A meta-analysis. *Oncology letters,* ***30****(3): 407*.
15. Zhao H and Li H (2019) Meta-analysis of ultrasound for cervical lymph nodes in papillary thyroid cancer: Diagnosis of central and lateral compartment nodal metastases. *European J Radiology,* ***112****: 14-21*.
16. de Bondt RB, Nelemans PJ, Hofman PA, *et al.* (2007) Detection of lymph node metastases in head and neck cancer: a meta-analysis comparing US, USgFNAC, CT and MR imaging. *European J Radiology,* ***64****(2): 266-72*.
17. Valizadeh P, Jannatdoust P, Ghadimi DJ, *et al.* (2025) Predicting lymph node metastasis in thyroid cancer: systematic review and meta-analysis on the CT/MRI-based radiomics and deep learning models. *Clinical Imaging,* ***119****: 110392*.
18. Iñarra Unzurrunzaga E, Gorriño Angulo M, Vidales Arechaga L, *et al.* (2011) Predictive ability of the CT to evaluate cervical lymph nodes in head and neck tumours. *Acta Otorrinolaringologica Espanola,* ***62****(6): 443-7*.
19. Zhan J, Diao X, Chen Y, *et al.* (2019) Predicting cervical lymph node metastasis in patients with papillary thyroid cancer (PTC) - Why contrast-enhanced ultrasound (CEUS) was performed before thyroidectomy. *Clinical Hemorheology and Microcirculation,* ***72****(1): 61-73*.
20. Luo ZY, Hong YR, Yan CX, *et al.* (2022) Utility of quantitative contrast-enhanced ultrasound for the prediction of lymph node metastasis in patients with papillary thyroid carcinoma. *Clinical Hemorheology and Microcirculation,* ***80****(1): 37-48*.
21. Suh CH, Baek JH, Choi YJ, *et al.* (2017) Performance of CT in the preoperative diagnosis of cervical lymph node metastasis in patients with papillary thyroid cancer: A systematic review and meta-analysis. *AJNR ,* ***38****(1): 154-61*.
22. Cho SJ, Suh CH, Baek JH, *et al.* (2019) Diagnostic performance of CT in detection of metastatic cervical lymph nodes in patients with thyroid cancer: a systematic review and meta-analysis. *European Radiology,* ***29****(9): 4635-47*.
23. Li QL, Ma T, Wang ZJ, *et al.* (2022) The value of contrast-enhanced ultrasound for the diagnosis of metastatic cervical lymph nodes of papillary thyroid carcinoma: A systematic review and meta-analysis. Journal of clinical ultrasound: *JCU,* ***50****(1): 60-9*.
24. Fan X, Zheng K, Chen W, *et al.* (2023) Ultrasonography features and American college of radiology thyroid imaging reporting and data system category in the prediction of central lymph node metastasis in papillary thyroid carcinoma. *Int J Radiat Res,* ***21****(4): 815*.
25. Hong YR, Luo ZY, Mo GQ, *et al.* (2017) Role of contrast-enhanced ultrasound in the pre-operative diagnosis of cervical lymph node metastasis in patients with papillary thyroid carcinoma. *Ultrasound in Medicine & Biology,* ***43****(11): 2567-75*.
26. Chen L, Chen L, Liu J, *et al.* (2020) Value of qualitative and quantitative contrast-enhanced ultrasound analysis in preoperative diagnosis of cervical lymph node metastasis from papillary thyroid carcinoma. *Journal of Ultrasound in Medicine,* ***39*** *(1): 73-81*.
27. Shi Z, Kuai M, Li B, *et al.* (2025) The role of VEGF in Cancer angiogenesis and tumorigenesis: Insights for anti-VEGF therapy. *Cytokine,* ***189****: 156908*.
28. Lorenc P, Sikorska A, Molenda S, *et al.* (2024) Physiological and tumor-associated angiogenesis: Key factors and therapy targeting VEGF/VEGFR pathway. *Biomedecine & Pharmacotherapie,* ***180****: 117585*.

[DOI: 10.61186/ijrr.24.2.21]

29. Leong SP, Pissas A, Scarato M, *et al.* (2022) The lymphatic system and sentinel lymph nodes: conduit for cancer metastasis. *Clinical & Experimental Metastasis,* ***39****(1): 139-57*.
30. Pimpalwar S, Chinnadurai P, Chau A, *et al.* (2018) Dynamic contrast enhanced magnetic resonance lymphangiography: Categorization of imaging findings and correlation with patient management. *European Journal of Radiology,* ***101****: 129-35*.
31. Zhang Y, Zhang X, Li J, *et al.* (2021) Contrast-enhanced ultrasound: a valuable modality for extracapsular extension assessment in papillary thyroid cancer. *European Radiology,* ***31****(7): 4568-75*.
32. Jiang J, Shang X, Zhang H, *et al.* (2014) Correlation between maximum intensity and microvessel density for differentiation of malignant from benign thyroid nodules on contrast-enhanced sonography. *Journal of Ultrasound in Medicine,* ***33****(7):1 257-63*.
33. Zhou Q, Jiang J, Shang X, *et al.* (2014) Correlation of contrast-enhanced ultrasonographic features with microvessel density in papillary thyroid carcinomas. *Asian Pacific Journal of Cancer Prevention: APJCP,* ***15****(17): 7449-52*.
34. Kaneko K, Abe K, Baba S, *et al.* (2010) Can calcification predict 131I accumulation on metastatic lymph nodes in papillary thyroid carcinoma patients receiving 131I therapy? Comparison of CT, 131I WBS and 18F-FDG PET/CT. *European Radiology,* ***20****(2): 477-83*.
35. Zoumalan RA, Kleinberger AJ, Morris LG, *et al.* (2010) Lymph node central necrosis on computed tomography as predictor of extracapsular spread in metastatic head and neck squamous cell carcinoma: pilot study. *The Journal of Laryngology and Otology,* ***124****(12): 1284-8*.
36. Lam J, Ying M, Cheung SY, *et al.* (2016) A Comparison of the diagnostic accuracy and reliability of subjective grading and computer-aided assessment of intranodal vascularity in differentiating metastatic and reactive cervical lymphadenopathy. *Ultraschall in der Medizin (Stuttgart, Germany : 1980),* ***37****(1): 63-7*.
37. Ni X, Xu S, Zhan W, *et al.* (2022) Ultrasonographic features of cervical lymph node metastases from medullary thyroid cancer: a retrospective study. *BMC Medical Imaging,* ***22****(1): 151*.
38. Zhang L, Li Y, Chen Z, *et al.* (2025) Diagnostic performance of dual-energy computed tomography (DECT) quantitative parameters for detecting metastatic cervical lymph nodes in patients with papillary thyroid cancer: A systematic review and meta-analysis. *European Journal of Radiology,* ***183****: 111917*.
39. Xue J, Li S, Qu N, *et al.* (2023) Value of clinical features combined with multimodal ultrasound in predicting lymph node metastasis in cervical central area of papillary thyroid carcinoma. *Journal of Clinical Ultrasound : JCU,* ***51****(5): 908-18*.
40. He Y, Qi X, Luo X, *et al.* (2023) Significance of magnetic resonance zoomed imaging with parallel transmission intravoxel incoherent motion imaging, ultrasonography and dual-energy computed tomography imaging in the differential diagnosis of benign thyroid nodule and papillary thyroid carcinoma. *Int J Radiat Res,* ***21****(3): 537*.
41. Zhao S, Yue W, Wang H, *et al.* (2023) Combined conventional ultrasound and contrast-enhanced computed tomography for cervical lymph node metastasis prediction in papillary thyroid carcinoma. *Journal of Ultrasound in Medicine,* ***42****(2): 385-98*.
42. Iqbal MA, Moazzam NF, Zhou H, *et al.* (2025) Integration of dual-source dual-energy CT quantitative parameters and ultrasound image features: A diagnostic method for extraglandular invasion of papillary thyroid carcinoma. *Oncology Letters,* ***30****(1): 356*.

[DOI: 10.61186/ijrr.24.2.21]